Jurnal Teknologi

Full paper

Indoor Air Conditioning Unit Air Flow Performance Study – Characterization of Cross Flow Fan Designs

New Mei Yet*, Vijay R. Raghavan, W.M. Chin

[a]*OYL R&D Centre Sdn. Bhd. Malaysia*

*Corresponding author: newmy@oyl.com.my

Article history

Received :15 June 2012
Received in revised form :12 August 2012
Accepted :28 August 2012

Graphical abstract

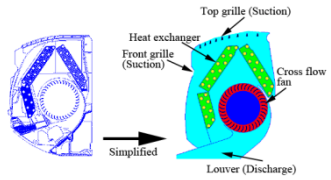

Abstract

A detailed characterization is carried out on a typical cross flow fan used in the Heating, Ventilation, and Air Conditioning (HVAC) industry, in order to understand the fan design in detail. The study is carried out numerically by use of the software FLUENT and followed by experimental validation. Appropriate grid size selection has done, the RMS error is less than 7%. From the study, it is concluded that the thickness of the blade determines the total flow area and flow rate delivered. When the internal blade angle is at 90°, shock free entry is incurred and maximum flow rate can be achieved. The external blade angle should be within 20 to 45 degrees, to avoid rapid drop of pressure coefficient and efficiency. Lastly, the formation of the eccentric vortex zone inside the cross flow fan and flow field pattern are observed. The forming location and size of the zone determines the total air flow rate delivered and the amount of flow leakage through the tongue. Thus, the efficiency of the fan is highly sensitive to the flow structure in this zone.

Keywords: Cross flow fan, air conditioning, computational fluid dynamics (CFD)

1.0 INTRODUCTION

The cross flow fan is a unique type of turbomachinery where the main flow moves transversely across the impeller, passing the blades twice. As shown in Figure 1, a common cross flow fan consists of several symmetrical sections. Each section has the same number of blades, blade profile, length, and blade orientation or arrangement. Unlike axial or centrifugal fans, a universal theory to design the cross flow fan used in the air conditioning unit could not be found because of the complex internal flow field with an eccentric vortex. This has makes it difficult to completely understand the flow characteristic of a cross flow fan. The cross flow fan flow characteristic is essential to improve its performance.

From the early work of Gabi and Klemm (2004), the performance characteristics of a cross flow fan depend more on the surrounding casing shape than on the design of the rotor and the blade grid. Shih *et al.* (2008) and Moon *et al.* (2003) have investigated the viscous effects due to the casing design. They concluded that the viscous effect will be more dominant when the overall system resistance increases. By resolving the viscous effect near the blades, an accurate prediction of the fan performance can be obtained. Besides that, it was noted in the study that an aperiodic fluctuating flow was found in the gap region between the rotating blades and the vortex wall.

The performance of the cross flow fan is not only affected by the casing design but also influenced by the design of cross flow fan itself. Lazzaretto (2003) has suggested that the ratio of impeller length to blade external diameter should not be lower than 1 to avoid strong border effect in and around the impeller. Meanwhile, the influence ratio of the blade internal diameter to external diameter is within the range of 0.7 to 0.85. Other works by Lazzaretto and his fellow researchers (2003, 2004), have revealed that the maximum flow rate can be achieved with internal blade angle of 90° and external blade angle of 25°. Internal blade angle is generally set at 90° to provide shock free entry in the second blade passage. Maximum pressure coefficient and efficiency decrease abruptly for external angles lower than 20^{o}.

The existence of the heat exchanger in air conditioning unit is generally neglected in most of the researchers' studies. As the heat exchanger contributed the major flow resistance to the system and the air flow passes through it first before entering the cross flow fan, it is reasonable to expect that the performance of the cross flow fan will be affected by it. In order to justify the performance of the cross flow fan with the existence of heat exchanger, the heat exchanger will be included in this work. The cross flow fan design parameters studied will then compared with results from previous study.

Figure 1 Typical example of cross flow fan and its cross sectional view

2.0 MUNERICAL MODELLING PROCEDURE

In this study, the simulation is in two dimensional (2D) and done on an indoor air conditioning unit model with several designs of cross flow fans. The main components of the model include a cross flow fan, heat exchanger, tongue, intake grilles, louver and casing as shown in Figure 2. All of the components remain the same throughout the study, except for the cross flow fan. The fluid domain is further extended to 1.5m x 1.5m to represent the room environment as shown in Figure 3. However, there is a wall in between the upstream and downstream domain to prevent that discharge air being sucked back from the front grille into the unit. This is to ease the air flow rate measuring process and accuracy. This geometry is modeled in the GAMBIT pre-processing software which is included along with the FLUENT 6.3 software package.

For the model, critical areas of flow such as the cross flow fan and heat exchangers are given denser mesh by generating the quad shaped meshes. Approximately 30 thousands numbers of quad elements are generated throughout the whole fluid domain. Figure 4 shows the meshes generated around a single blade of the cross flow fan. The inlet of the domain is defined as "pressure inlet" with static pressure equal to zero, while the outlet is defined as "pressure outlet". The rest of the boundary is defined as wall, interior, and interface. The heat exchanger is simplified as a porous medium and the cross flow fan is treated as rotating zone by using the sliding mesh approach.

As the fan is rotating, the time will be changing as well; therefore, the simulation needs a transient (unsteady state) approach. Due to the high speed cross flow fan and changing air flow profile from time to time, the flow is always unsteady and turbulent. In order to solve the turbulent flow, the standard *k*-epsilon model has been applied. Initial turbulence kinetic energy and turbulence energy dissipation rate of 1 m^2/s^3 are set. Enhanced wall treatment has been selected with zero velocity condition. Incompressible flow has been assumed.

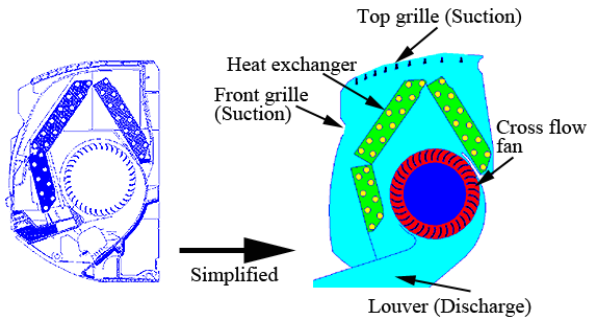

Figure 2 The cross section view of the typical indoor air conditioning unit and the simplified 2D simulation model

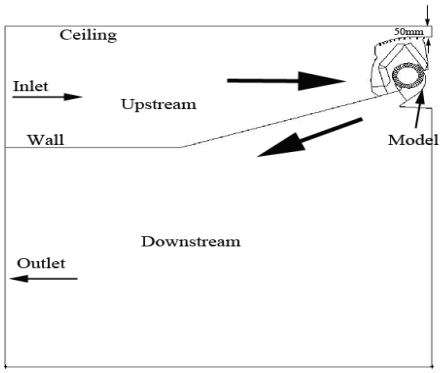

Figure 3 The simulation domain (1.5m x 1.5m) and model set up

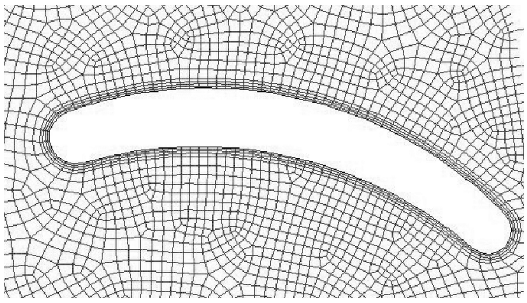

Figure 4 Mesh generated around the blade for 2D model

2.1 Grid Size Selection

The grid size used in a particular simulation is very important as it will significantly affect the results if an inappropriate size is used. Therefore, the grid size selection is essential for simulation within acceptable accuracy with the least computing resources. Six different mesh sizes have been employed in the rotating zone to test the simulation accuracy as tabulated in Table 1. From the table, the lowest deviation between numerical and experimental results with the tested air flow rate is 691.05 cubic feet per minute (CFM), of 4.06%, occurred with a mesh size of 0.1mm. But this model required 5 days to achieve a converged solution.

In addition, a plot of the deviation error and time to converge is shown against the mesh size in the following Figure 5. The intersection point of the two trend lines is shown at a mesh size of 0.23mm with a convergence time of at least 2.5 days and with a deviation error of about 8%. This is acceptable as it takes less time than that for a mesh size of 0.1mm. At the same time, the comparison of flow rate between simulation and experimental results showed a deviation of 6.49% with a mesh size of 0.2mm. In view of the savings in computing time, the mesh size of 0.2mm with 6.49% of error and 2.8 days of convergence time is selected.

Table 1 Simulation results for six different mesh sizes

Mesh size (mm)	Air Flow Rate (CFM)	% of Error	Time (Days)
0.1	662.98	4.06	5.0
0.2	646.19	6.49	2.8
0.3	611.48	11.51	2.1
0.4	597.63	13.52	1.4
0.5	591.98	14.34	0.8
0.6	583.58	15.55	0.4

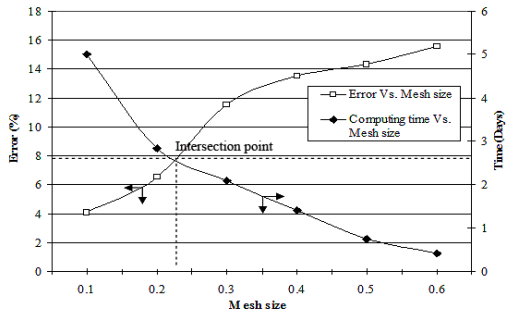

Figure 5 Intersection point between percentage of deviation error and time required for convergence

3.0 EXPERIMENTAL PROCEDURE

For validation purpose, an experiment was carried out in an air nozzle flow test chamber (Figure 6) which complies with the requirements of American Society of Heating, Refrigerating, and Air Conditioning Engineers (ASHRAE) Standard 51, 1999. All the measuring instruments were calibrated in-house with standard calibration equipment. The schematic diagram of the test rig is illustrated in Figure 7. Air straighteners have been installed before and after the nozzles to dampen flow turbulences which could affect the nozzle pressure drop readings. When the test unit is turned on, the speed of the motor in the test unit is adjusted from 800 to 1300 RPM to obtain the required air flow rate. The chamber blower speed is adjusted accordingly until the external static pressure reading equals zero. This blower will accommodate the losses due to the chamber itself.

The air conditions such as wet and dry bulb temperatures were taken by using temperature sensors (RTD). For each test, three sets of readings are captured by a data logger with a one-minute interval between the readings. The average values of the readings are then converted into CFM by using the equation (1) given below. The result is recorded in a data sheet as in Table 2. The result from the experiment is then compared with the simulation results.

$$Q = A_{Nozzles} \times C_D \times \sqrt{2 \times \Delta p \times S_p V} \quad (1)$$

Where

Δp	Pressure drop
C_D	Coefficient of discharge, which is dependent on the air Reynolds number
$S_P V$	Air specific volume which is dependent on the air conditions (dry and wet bulb temperatures)

Figure 6 The air flow chamber

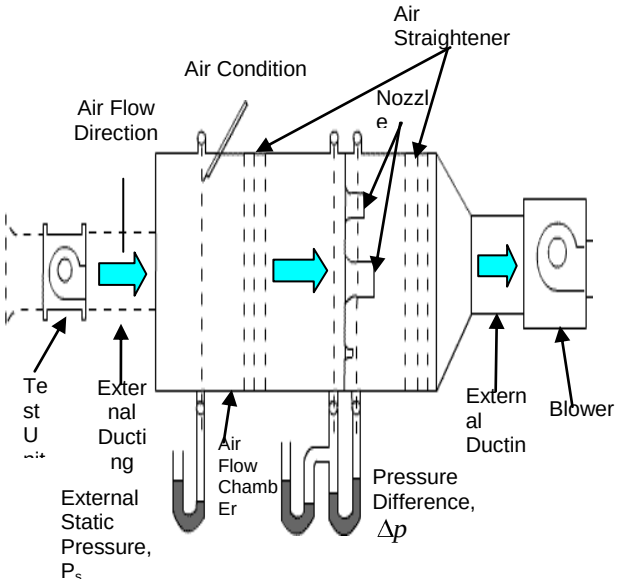

Figure 7 Schematic diagram of test rig setup

3.1 Validation

The same magnitudes of revolutions per minute (RPM) from the experimental results are inputted into the numerical model, and the results are compared with the experimental results as shown in Figure 8. It is observed that the errors are consistently within 6.5%. These differences can be explained as in 2D numerical model, the 3D geometrical effects are no accounted. In view of this, the difference of 6.5% between the experimental and numerical results is accepted and the numerical model is therefore deemed to be validated and may be used with other configurations.

4.0 RESULT AND DISCUSSION

In order to characterize the cross flow fan performance, four types of cross flow fans that are currently available in the market have been selected. These four fans were selected due to their high volume of usage and also the variability of the blade profiles. For convenience, these four fans are labeled as F1 to F4, as shown in Figure 9.

Figure 10 shows that volumetric flow rate produced by each of the cross flow fans at different rotational speeds. The flow rate for fan F4 is the highest while F2 has the lowest flow rate. From Table 3, F2 has the thickest (2.89mm) blade while F3 has the thinnest (1.52mm) blade. The volumetric flow rate of F2 is the least, where the flow area is being restricted by the blade thickness. It is deduced that narrower shapes will give more space for the air flow to pass through, while a wider shape will restrict the air flow passage as the overall flow area become less. However, in comparing F4 with F3, both of which have similar shape and profile, the flow rate of F4 is much larger than that of F3, though F3 has a thinner blade profile. This could be due to the difference of the other parameters, such as the internal and external blade angles, diameter, and blade thickness (Figure 11).

Table 2 Air flow test data sheet

DESCRIPTION	EVAP. COIL : CONDITION DRY					
F/M SPEED (RPM)	1	2	3	4	5	6
STATIC PRESSURE(mmAq)	0.00	0.00	0.00	0.00	0.00	0.00
VOLTAGE, V / FREQ.(Hz)/PH.	227.3/50/1	188.2/50/1	206.0/50/1	174.4/50/1	187.0/50/1	172.5/50/1
POWER FACTOR,%	0.999	0.995	0.996	0.988	0.999	1.000
AMPERE, A	0.295	0.278	0.233	0.267	0.218	0.204
POWER, W	67.0	52.0	47.7	46.0	40.7	35.2
RPM, REV/MIN	1275	1133	1084	1004	952	870
AIR LEAVING DB °C	30.4	30.5	30.6	30.4	30.3	30.1
AIR LEAVING WB, °C	21.6	22.2	22.4	22.9	22.3	21.9
DIFF.PRESSURE, dp (mmAq)	47.39	64.46	57.87	51.24	46.15	36.60
S NOZZLE DIAMETER(d) m	0.11981	0.10160	0.10160	0.10160	0.10160	0.10160
S NOZZLE AREA (A) m²	0.0112685	0.0081032	0.0081032	0.0081032	0.0081032	0.0081032
SPV	0.8756	0.8772	0.8778	0.8785	0.8770	0.8757
V = SQRT (2g X dp X SpV)	28.53	33.31	31.57	29.72	28.18	25.08
Re = rV(Sd)/ μ	208614	206095	195157	183649	174485	155575
Cd	0.99	0.99	0.98	0.98	0.98	0.98
V' = Cd X V	28.25	32.97	30.94	29.12	27.62	24.57
Q = A X V' X 60 (CMM)	19.50	17.03	15.84	14.76	13.73	12.15
CFM = Q X 35.3	691.05	605.83	561.64	525.36	488.42	433.36
SCFM	667.04	584.80	542.13	507.10	471.40	412.30

PHYSICAL CONSTANTS USED IN CALCULATION:

GRAVITATIONAL FORCE, g = 9.81 m/s²

Re	Cd
50 000 ~ 100 000	0.97
100 000 ~ 200 000	0.98

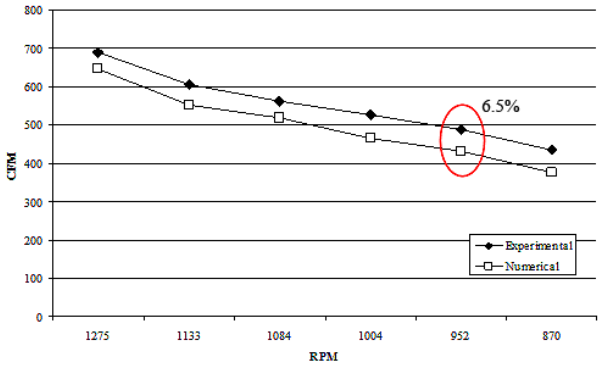

Figure 8 Comparison between experimental and numerical results

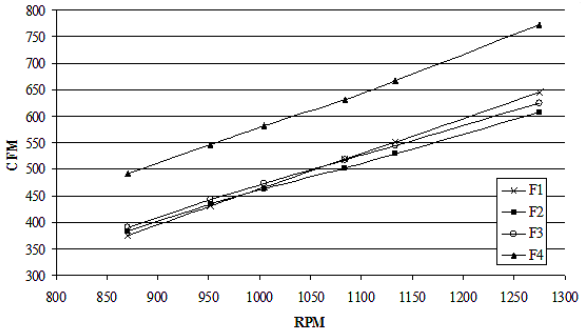

Figure 10 Comparison of volumetric flow rate (CFM) between four different fans

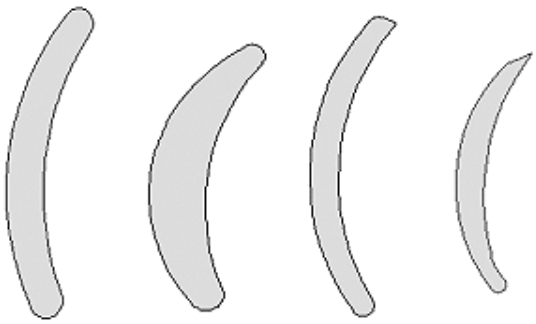

Figure 9 Sketch of the blade profiles used in the study

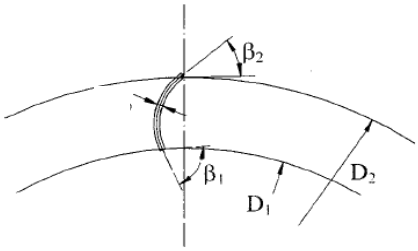

Figure 11 Illustration of the parameter involved in blade design (Lazzaretto, 2003)

Table 3 Geometry analysis for each blade profile

Blade	Flow area (m^2)	Internal diameter D1 (mm)	External diameter D2 (mm)	Thick-ness t (mm)	Internal angle β1 (°)	External angle β2 (°)	Ratio D1/D2
F1	0.00410	81.41	108.05	1.78	79.83	42.50	0.75
F2	0.00322	82.97	108.70	2.89	83.34	22.34	0.76
F3	0.00411	77.63	108.00	1.52	88.28	35.87	0.72
F4	0.00447	87.75	108.33	1.61	89.06	30.02	0.81

The effect of the fan diameter is usually examined by using the ratio of internal to the external diameters (D1/D2), where the optimum range should be within the range of 0.7 to 0.85 (Lazzaretto, 2003). All the four fan blades simulated in this work have their diameter ratios falling within this range. At this range, the influence is considered negligible. Based on Lazzaretto (2003), the best performance is for the internal and external blade angles of 90º and 25º, respectively. This is again shown to agree in this study where the internal blade angle for F4 is 89º, which is close to 90º, where its performance is the highest among the four cross flow fans.

4.1 Eccentric Vortex Zone

On the other hand, zero relative velocity has been observed at the lower part of the through flow region (Figure 12), where the air re-circulates and does not discharge out. Low static pressure is also observed at the same position (Figure 13). This region is called the eccentric vortex region. Formation of the eccentric zone can be observed clearly from the velocity vector plot shown in Figure 14 where the air is re-circulated within the zone. The air follows the circulatory flow path and discharges after passing through the blades a second time. Eccentric vortex zone is the most important parameter to determine the functionality of the cross flow fan. The position and formation of the eccentric vortex is very important as it not only affects the flow rate, but also the total pressure drop and noise performance of the fan.

The gap between the tongue and fan also affects the flow rate because the gap allows some of the air to back flow, instead of being discharged out of the impeller. This can be seen in Figure 15. Improper tongue design will affect the efficiency of the fan as bigger gap allows more air to back flow and eventually push the eccentric vortex zone to higher position. Thus it will reduce the amount of air flow delivered. The gap between the tongue and fan should be kept as minimum as possible to obtain the maximum flow rate.

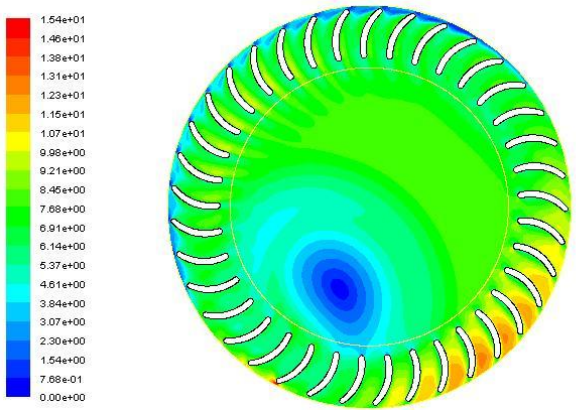

Figure 12 Velocity contour plot of fan F1

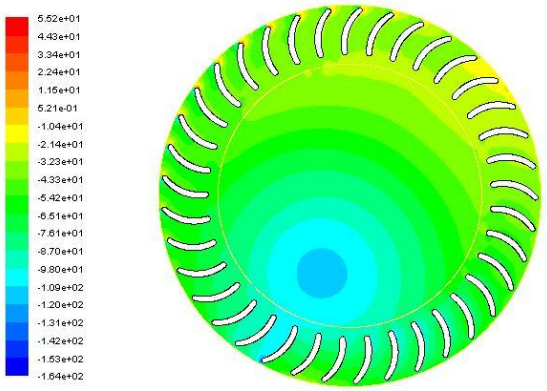

Figure 13 Pressure contour plot of fan F1

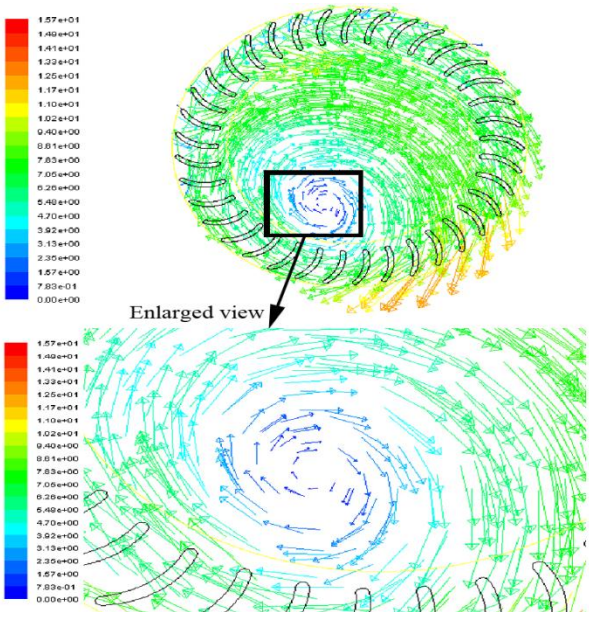

Figure 14 The velocity vector plot inside the cross flow fan and enlarged view of the eccentric vortex region

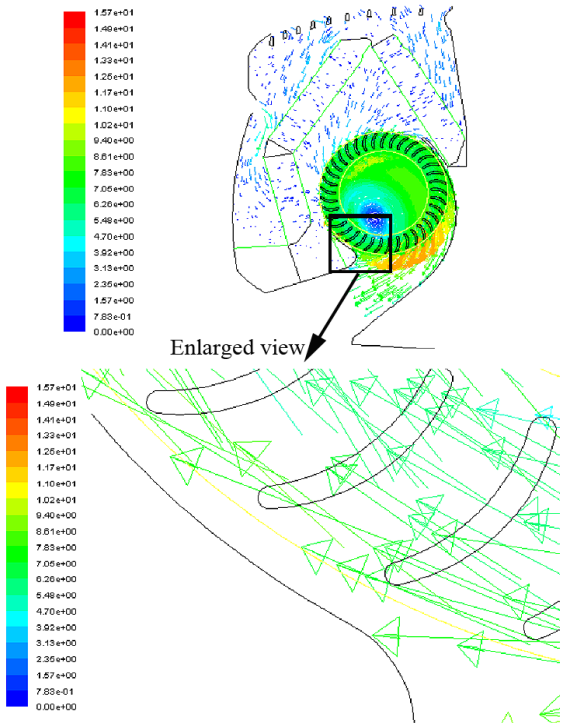

Figure 15 The velocity vector plot of the whole model and enlarged view of the gap between tongue and fan

4.2 Casing Design

The next parameter that will affect the performance of the cross flow fan is the casing design. From the velocity contour plots for three different unit casing designs (unit A, B and C in Figure 16), but with the same cross flow fan and heat exchanger, a significant difference in the location of the eccentric vortex zone can be clearly seen. The size and position of the eccentric vortex zone will affect the total air flow rate delivered by the fan. The larger eccentric vortex zone creates more recirculation within the fan which reduces the air discharge from the unit. The eccentric vortex zone should be kept at the lowest part of the fan, and as close as possible to the blade and tongue. This is to minimize the reversal of flow and at the same time maximize the air flow delivered.

Besides that, the suction effect on the heat exchanger due to the cross flow fan will leads to maldistribution phenomenon. From Figure 16, it is also clearly seen that the air flow is maldistributed on the surfaces of the heat exchanger of all three models. To quantify the effect of maldistribution, the standard deviation of the tangential velocity on the inlet of the heat exchanger is used. The standard deviation will indicate the deviation from uniformity of the air flow distribution. Lower values of the standard deviation indicate that the air flow distribution is more uniform. Meanwhile, a higher standard deviation shows higher maldistribution.

The standard deviation is calculated for every node at each heat exchanger inlet by using equation (2). A combined average standard deviation for the three sections of the heat exchanger can be calculated with the mass-weighted standard deviation by using equation (3) as follows.

Standard deviation of each heat exchanger (j = 1, 2, and 3):

$$d_j = \left(\frac{\Sigma \; X_i - \bar{X}^{\;2}}{n} \right)^{\frac{1}{2}} \tag{2}$$

Mass-weighted averaged standard deviation:

$$d_m = \frac{d_1\dot{m}_1 + d_2\dot{m}_2 + d_3\dot{m}_3}{\dot{m}_1 + \dot{m}_2 + \dot{m}_3} \tag{3}$$

Where

d_j	Standard deviation for each heat exchanger
d_m	Mass-weighted average standard deviation
$\dot{m}$	Mass flow rate of the particular heat exchanger
n	Number of nodes
X_i	Average tangential velocity magnitude
$\bar{X}$	Tangential velocity magnitude for each node on the heat exchanger surface

The results of the velocity standard deviation are shown in Table 4. From the table, Unit B and C have lower standard deviation as compared to unit A. This means that the casing with top intake (unit B and C) will deliver more uniform air flow to the heat exchangers as compared to casing A with both front and top intakes. For unit B and C, the air flow is supplied from a single intake at which the air is almost at constant uniform velocity. Therefore, as the air is only supplied from the top, the lower part of the heat exchanger will have insufficient air flow supply and it will be detrimental to the heat transfer process. In this case, the heat exchanger will not be fully utilized

On the other hand, for unit A with both air intakes, the front intake area is very narrow and therefore, higher velocity air flow is supplied compared with top intake air velocity. These two streams of air flows are mixed upon entering the unit which caused uneven air velocity and pressure drop. The non-uniform air flow distribution will affect the heat transfer process and thereby, lower the cooling capacity. Therefore, the maldistribution effect should take into consideration when doing casing design. A more uniform air flow distribution enhances the heat transfer of the heat exchanger, and thus, improves the overall performance of the unit.

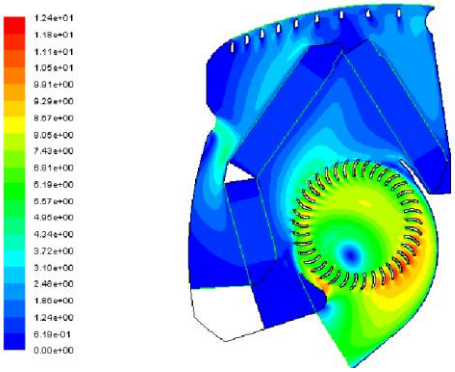

Figure 16a Unit A

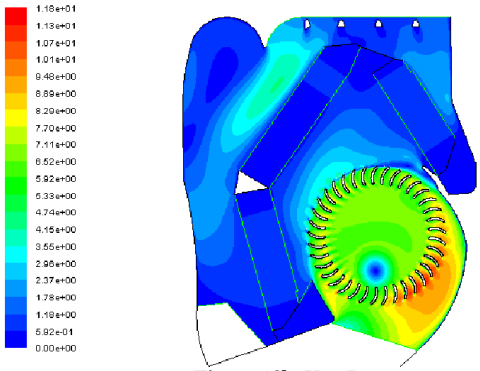

Figure 16b Unit B

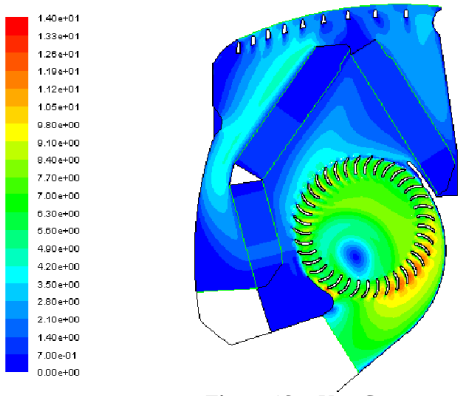

Figure 16c Unit C

Figure 16a, 16b and 16c Velocity contour plots for 3 different casing designs with the same cross flow fan

Table 4 Total mass-weighted average standard deviation value for each unit

Unit	Standard Deviation			Mass Flow Rate (Kg/s)			Mass-Weighted Average			Total
	Hx 1	Hx2	Hx3	Hx1	Hx2	Hx3	Hx1	Hx 2	Hx 3	
A	2.15	0.50	0.87	0.18	0.39	0.38	0.40	0.20	0.35	0.95
B	1.64	0.40	0.28	0.21	0.23	0.29	0.48	0.13	0.11	0.71
C	0.93	0.33	0.84	0.27	0.35	0.45	0.24	0.11	0.36	0.70

5.0 CONCLUSION

The results obtained from the simulation agreed coherently with theory, experimental data, and results of the previous studies. The study here clearly has shown that each design parameter of the cross flow fan influences the performance of the air conditioning unit. The following parameters are summarized as below:

(i) The best performances for internal and external blade angles are at 90º and 25º, respectively.

(ii) The effect of the fan diameter is examined by using the ratio of internal to the external diameters (D1/D2) where the optimum range should be within the range of 0.7 to 0.85.

(iii) It is deduced that narrower shapes will give more space for the air flow to pass through while a wider shape will restrict the air flow passage as the overall flow area become less.

(iv) The formation and position of the eccentric vortex zone will affect the air flow rate delivered by the particular cross flow fan.

(v) The gap between the tongue and fan moderately affect the flow rate because the gap allows some reverse air flow instead of being fully discharged out of the impeller.

(vi) Improper design of casing affects the performance of the heat exchangers and eventually, affects the heat duty of the air conditioning unit.

Acknowledgement

This study has been supported by O.Y.L. R&D Centre Sdn. Bhd., Malaysia and is gratefully acknowledged.

References

[1] Ahmad ASHRAE Standard 51. 1999. Laboratory Methods of Testing Fans for Aerodynamic Performance Rating, American Society of Heating, Refrigerating and Air-Conditioning Engineers.

[2] Gabi M., and Klemm, T. 2004. Numerical and Experimental Investigations of Cross-Flow Fans. *Journal Computational and Applied Mechanics*. 5: 251–261.

[3] Lazzaretto, A. 2003. A Criterion to Define Cross-flow Fan Design Parameters. *Journal Fluids Engineering*. 125: 680–683.

[4] Lazzaretto, A., Toffolo, A., and Martegani, A. D. 2003. A Systematic Experimental Approach to Cross-flow Fan Design. *Journal Fluids Engineering*. 125: 684–693.

[5] Moon, Y. J., Cho, Y., and Nam, H-S. 2003. Computation of Unsteady Viscous Flow and Aero Acoustic Noise of Cross Flow Fan. *Computers and Fluids*. 32: 995–1015.

[6] Shih, Y.-C., Hou, H.-C., and Chiang, H. 2008. On Similitude of the Cross Flow Fan in A Split-Type Air Conditioner, Applied Thermal Engineering. 28: 1853–1864.

[7] Toffolo, A., Lazzaretto, A., and Martegani, A. D., 2004. Cross-Flow Fan Design Guidelines for Multi-Objective Performance Optimization. *Journal Power and Energy*. 218: 33–42.